ACCEPTED MANUSCRIPT

PLEASE CITE THIS ARTICLE AS DOI: 10.1063/5.0091521

Journal of Applied Physics

AIP Publishing

Von Kármán spatial correlation function to describe wave propagation in polycrystalline media

Andrea P. Argüelles[1, a)]

Department of Engineering Science and Mechanics, The Pennsylvania State University, University Park, PA 16802, USA

(Dated: 17 May 2022)

Analytical functions that describe the spatial heterogeneity in polycrystalline media are highly desirable. These mathematically tractable descriptors can be readily implemented in physical models of static and dynamic material behavior, including wave propagation. This paper explores the suitability of von Kármán spatial correlation functions (SCF) to describe polycrystalline media with a distribution of grain sizes. The empirical two point statistics are compared to the von Kármán and other commonly reported SCFs. The von Kármán function is shown to be more accurate than the exponential function, and more tractable that the sum of exponentials form. The impact of the SCF on wave propagation and scattering is studied by employing a well-defined analytical model for attenuation. The attenuation varies by over a factor of two for the aluminum case considered. These results provide preliminary insights into the suitability of a closed-form von Kármán SCF to describe polycrystalline media with increasingly complex microstructures.

[a)]arguelles@psu.edu

ACCEPTED MANUSCRIPT

PLEASE CITE THIS ARTICLE AS DOI: 10.1063/5.0091521

Journal of Applied Physics

AIP Publishing

I. INTRODUCTION

Microstructure is known to directly impact the physical properties of heterogeneous materials. In general, the structure is characterized by simple metrics such as average grain size and shape. However, these approaches fail to capture sufficient details to enable reconstruction of the original microstructure. These intricate variations may also affect dynamic parameters associated with wave propagation such as attenuation[1] and nonlinearity.[2] The material microstructure can be more rigorously characterized by using n-point spatial correlations. In their simplest form, one-point correlations capture the volume fractions of constituent phases. A single order increase in complexity through two-point correlations, the spatial distribution of heterogeneities in the microstructure can be captured. Most importantly, these two-point correlations have proved useful in reconstructing the original microstructure[3], which is a critical step in design for performance optimization.[4]

Different approaches have been explored to obtain these spatial statistics. At the forefront of these efforts was Berryman[5], who presented a digital image processing approach to calculate one-, two- and three-point correlations. In more recent years, Kalidindi et al.[6] have significantly contributed to the identification of critical features from microstructural images and their representation as spatial correlations. For example, Altschuh et al.[7] explored data science approaches for feature identification. As previously mentioned, these empirical representations of the microstructure have shown to be critical in predicting properties and performance.[3,4,8] However, a gap in accurately connecting these efforts to other methods of microstructure characterization remains.

More specifically, the nondestructive characterization of polycrystalline media through ultrasonic methods has seen significant advances in recent years. For example, recent advances have linked ultrasonic attenuation to stress and strain in polycrystals.[9] However, most analytical models of ultrasonic attenuation and scattering, rely on mathematically tractable functions to describe the propagation medium. Initial models of wave propagation in polycrystalline media assumed an exponential form for the two point correlations (or spatial correlation functions), which relied on Poisson statistics to describe the cord lengths.[10] Later models enabled introduction of other analytical functions to represent the spatial statistics[11,12], but they still elected the exponential form given the simplicity of its power spectrum. More recently, these models have been expanded to include a distribution of sizes

ACCEPTED MANUSCRIPT

PLEASE CITE THIS ARTICLE AS DOI: 10.1063/5.0091521

Journal of Applied Physics

AIP Publishing

through analytical functions[1] while others have explored the use of synthetic polycrystals to describe the spatial statistics in polycrystals with equiaxed[13–16] and irregular[17,18] grains. However, comparisons to analytical models when using synthetic media rely on overdetermined fitting functions to represent the empirically obtained spatial statistics. Tractable, analytical forms of the two point spatial correlation function are still a significant gap, as many inversion efforts still rely on simple parameters such as grain size.[19,20]

Here, we explore the use of a von Kármán spatial correlation function (SCF) to describe the morphology of grains in polycrystalline media. The von Kármán SCF has been used in geoscience to describe velocity inhomogeneities in the earth,[21,22] a highly complex heterogeneous medium. However, its suitability to describe polycrystalline microstructures, such as those found in metals, at ultrasonic frequencies has yet to be explored. The paper is organized as follows: Section II presents the theoretical framework for the spatial correlation function beginning with the conventional exponential approach and the details of the von Kármán option. In addition, a model for elastic wave attenuation is presented. Section III evaluates the feasibility of the various correlation functions to describe the spatial statistics of synthetic polycrystals with a distribution of grain sizes. Synthetic microstructures are generated using DREAM.3D given the increased accuracy in representing grain structures when compared to other tessellation approaches.[23] The results are expanded to describe the impact on longitudinal and shear ultrasonic attenuation when compared to other commonly used analytical representations of the two point statistics.

II. THEORY

Heterogeneity in polycrystalline media can be described using statistical parameters pertaining to the fluctuations from the mean response. For example, we may define $\delta\mathbf{C}$ as the modulus fluctuations about the average elastic modulus $\langle\mathbf{C}\rangle$ such that the covariance function given by[24]

$$\Lambda_{ijkl}^{\alpha\beta\gamma\delta}\left(\mathbf{x},\mathbf{x}'\right)=\langle\delta C_{ijkl}\left(\mathbf{x}\right)\delta C_{\alpha\beta\gamma\delta}\left(\mathbf{x}'\right)\rangle, \tag{1}$$

contains all relevant statistical information regarding the inhomogeneity. Statistical homogeneity, where the covariance is dependent only on the distance between $\mathbf{x}$ and $\mathbf{x}'$, $\mathbf{r}=\mathbf{x}-\mathbf{x}'$, is commonly assumed. Further, when the crystallites are randomly oriented, the spatial and

ACCEPTED MANUSCRIPT

PLEASE CITE THIS ARTICLE AS DOI: 10.1063/5.0091521

Journal of Applied Physics

AIP Publishing

tensorial components are decoupled, yielding

$$\Lambda_{ijkl}^{\alpha\beta\gamma\delta}(\mathbf{r}) = \Xi_{ijkl}^{\alpha\beta\gamma\delta} W(\mathbf{r}), \tag{2}$$

where $\Xi_{ijkl}^{\alpha\beta\gamma\delta}$ is the eighth-rank covariance of the elastic modulus tensor and $W(\mathbf{r})$ is the two point spatial correlation function (SCF), which gives a statistical measure of the spatial scale of the heterogeneity. Here, the SCF denotes the probability that two points separated by a distance r lie within the same crystallite (or grain). Empirically, this probability may be defined as[14]

$$W(r) = \frac{1}{N_p} \sum_{n=1}^{N_p} I(x_n, x_n + r) \tag{3}$$

where I equals 1 when positions x_n and $x_n + r$ lie in the same grain and zero otherwise. Modeling efforts of the medium's response often necessitate analytical representations of the heterogeneity. To this end, in Sec. II A, we define mathematically tractable SCFs that may be used to describe polycrystalline media. Then, in Sec. II B, the power spectral densities of the SCFs are implemented to define the attenuation of said media.

A. Spatial Correlation Function

Statistical approaches enable us to treat heterogeneous media as a continuum. In the geophysical literature, Earth heterogeneities are commonly described using the von Kármán SCF[25,26]. This model describes the medium using two parameters as follows[22]

$$W(r) = \frac{2^{1-\kappa}}{\Gamma(\kappa)} \left(\frac{r}{L}\right)^{\kappa} K_{\kappa}\left(\frac{r}{L}\right) \tag{4}$$

where $\Gamma(\kappa)$ is the gamma function, K_κ is the modified Bessel function of the second kind of order κ, L is the correlation length, related to the typical size of heterogeneities (or grains in the polycrystalline case), and κ is the Hurst number ($0 \leq \kappa \leq 1$), related to the "roughness" of the medium.[27] With increasing Hurst number, von Kármán media display smoother spatial variations. A value of $\kappa = 0$ corresponds to a smooth Euclidean field, while $\kappa = 1$ represents a space-filling medium. Because the Hurst number is associated with the fractal dimension of a stochastic field, it may be suitable for representing complex physical features in polycrystalline microstructures.

A special case of Eq. (4) occurs when $\kappa = 0.5$,

$$W(r) = e^{-r/L}. \tag{5}$$

ACCEPTED MANUSCRIPT

PLEASE CITE THIS ARTICLE AS DOI: 10.1063/5.0091521

Journal of Applied Physics

AIP Publishing

This exponential form of the SCF was shown to be physically realizable by Torquato[28,29] and is commonly employed to describe wave propagation in polycrystalline media given the simplicity of its spectral representation, first shown by Stanke and Kino[12]. The exponential SCF assumes the cord lengths describing the spatial statistics of the microstructure have Poisson statistics. Further, this form of the SCF assumes that the microstructure can be described by a single characteristic length, L. Others have attempted to capture the microstructural complexities of polycrystals with a distribution of grain sizes by considering a weighted sum of exponential functions as follows[30]

$$W(r) = \sum_{i=1}^{N} A_i e^{-r/L_i} \tag{6}$$

where A_i and L_i are fitting coefficients of the measured two point statistics for a polycrystal and N is the number of terms in the sum. Van Pamel et al.[30] specify that individual terms of the series do not hold physical meaning (e.g., the individual A_i coefficients may be negative). However, physical constraints are imposed on the sum such that $\sum_{i=1}^{N} A_i = 1$. Others have attempted to attribute physical meaning to the weighting coefficients by linking to the volume fraction of the individual grain sizes[1]. Yet, least squares fitting of the resulting integral expressions is challenging. In this paper, we evaluate the validity of the von Kármán, exponential, and summed exponential correlation functions to describe the morphology of polycrystalline media.

B. Ultrasonic Attenuation

Based on the theory of Weaver[11], we may write the longitudinal and shear attenuation in a polycrystalline medium as

$$\begin{aligned} \alpha_L &= \alpha_{LL} + \alpha_{LT}, \\ \alpha_T &= \alpha_{TT} + \alpha_{TL}, \end{aligned} \tag{7}$$

respectively, where α_{ij} represent the contributions of longitudinal, L, and shear/transverse, T, scattering modes. The first index corresponds to the incident wave, while the second

ACCEPTED MANUSCRIPT

PLEASE CITE THIS ARTICLE AS DOI: 10.1063/5.0091521

Journal of Applied Physics

AIP Publishing

index corresponds to the scattered wave mode. These contributions are explicitly given by

$$\begin{aligned}
\alpha_{LL} &= \frac{k_L^4 \pi}{4\rho^2 c_L^4} \int \tilde{\eta}\left(\theta_{ps}\right) L\left(\theta_{ps}\right) \sin\theta_{ps} d\theta_{ps} \\
\alpha_{LT} &= \frac{k_T^4 \pi}{4\rho^2 c_L^3 c_T} \int \tilde{\eta}\left(\theta_{ps}\right) \left[M\left(\theta_{ps}\right) - L\left(\theta_{ps}\right)\right] \sin\theta_{ps} d\theta_{ps} \\
\alpha_{TL} &= \frac{k_L^4 \pi}{8\rho^2 c_T^3 c_L} \int \tilde{\eta}\left(\theta_{ps}\right) \left[M\left(\theta_{ps}\right) - L\left(\theta_{ps}\right)\right] \sin\theta_{ps} d\theta_{ps} \\
\alpha_{TT} &= \frac{k_T^4 \pi}{8\rho^2 c_T^4} \int \tilde{\eta}\left(\theta_{ps}\right) \left[N\left(\theta_{ps}\right) - 2M\left(\theta_{ps}\right) + L\left(\theta_{ps}\right)\right] \sin\theta_{ps} d\theta_{ps}
\end{aligned} \tag{8}$$

where L, M, and N are related to the inner products of the covariance with the propagation ($\hat{\mathbf{k}}$) and displacement ($\hat{\mathbf{e}}$) directions ($\hat{k}'_\alpha \hat{k}_\delta \hat{e}'_\beta \hat{e}_\gamma \hat{k}'_l \hat{k}_m \hat{e}'_j \hat{e}_k \Xi^{\alpha\delta\beta\gamma}_{lmjk}$). These terms were explicitly defined by Kube and Turner[31] for a statistically isotropic medium with crystallites of arbitrary symmetries. Weaver's[11] derivation is employed herein as it accounts for spatial variations in the microstructure through its use of an SCF. Unlike the solution presented by Stanke and Kino[12], Weaver ignores phase velocity dispersion to obtain explicit expressions for the attenuation coefficients, limiting the applicability to the Rayleigh and stochastic frequency regimes. Exceptions to the equivalency between Stanke and Kino[12] and Weaver's[11] models were presented by Kube[32].

The final term to define in Eq. (8) is the heterogeneity power spectrum, given by the spatial Fourier transform of the SCFs defined in Sec. II A. We first consider the power spectrum for the von Kármán SCF,

$$\tilde{\eta}(k) = \frac{\pi^{1/2}\Gamma\left(\kappa + 3/2\right) L^3}{\Gamma(\kappa)\left(1 + k^2 L^2\right)^{\kappa+3/2}}, \tag{9}$$

which for the exponential function, when $\kappa = 0.5$, simplifies to

$$\tilde{\eta}(k) = \frac{L^3}{\left(1 + k^2 L^2\right)^2}. \tag{10}$$

We may write this more generally as a function of the angle between the incident and scattered waves θ_{ps} as

$$\tilde{\eta}(\theta_{ps}) = \frac{L^3}{\pi^2\left[1 + L^2\left(k^2 + k'^2 + 2kk'\cos\theta_{ps}\right)\right]^2}, \tag{11}$$

where k and k' are the wave numbers for the incident and scattered waves, respectively. The von Kármán spectrum may be written analogously. Note that for the summed exponentials SCF, the power spectrum may be written as a sum of Eq. (11) over all terms in the function.

ACCEPTED MANUSCRIPT

PLEASE CITE THIS ARTICLE AS DOI: 10.1063/5.0091521

Journal of Applied Physics

AIP Publishing

III. RESULTS

Microstructural complexity can take many forms in polycrystalline media. Here, the applicability of the von Kármán SCF is tested on synthetic microstructures with varying grain size distributions, known to impact the linear[1] and nonlinear[2] ultrasonic response of polycrystals. First, the fitting error for the three analytical functions presented in Sec. II A is evaluated as a function of grain size distribution width. Then, the resulting correlation lengths are compared to the spatial statistics for the corresponding microstructures. Finally, the different analytical fits are employed to calculate longitudinal and shear ultrasonic attenuation and the resulting differences are discussed.

A. Synthetic Polycrystalline Microstructures

Four 1 mm^3 volumes were generated in DREAM.3D[23] through the Pennsylvania State University's Institute for Computational and Data Sciences' Roar supercomputer using the sample pipeline provided by Norouzian and Turner[14]. The input mean grain diameter was 30 μm and the standard deviation varied from 6 to 21 μm, expected to result in log-normal distribution widths ranging from $0.25 < \sigma < 1$. The output statistics for the grain size distributions for each of the generated volumes are provided in Table I, where μ and σ are the unbiased estimates of log-normal distribution parameters (i.e., the mean and standard deviation of logarithmic values, respectively). Note that the last two cases did not strictly follow a log-normal distribution because a large number of small grains were present to ensure volume filling. Because the total volume of the synthetic microstructures was fixed, the total number of grains decreased with increasing distribution width, σ. Sample cross sections of each microstructure are given in Fig. 1.

FIG. 1. Sample 1 mm x 1 mm cross sections for synthetic polycrystalline microstructures with increasing standard deviations of 6.87, 12.72, 16.74, and 20.59 from left to right.

A subroutine to calculate the SCF empirically was implemented in MATLAB (R2021b). The microstructural data, along with the aforementioned statistics, was exported from

ACCEPTED MANUSCRIPT

PLEASE CITE THIS ARTICLE AS DOI: 10.1063/5.0091521

Journal of Applied Physics

AIP Publishing

TABLE I. Output statistics for the grain size distribution parameters for synthetic microstructures generated using DREAM.3D.

μ	σ	Mean (μm)	Standard Deviation (μm)	Number of Grains
3.37	0.23	29.96	6.87	60905
3.36	0.41	31.41	12.72	37235
3.23	0.63	29.94	16.74	33221
3.07	0.87	29.01	20.59	26073

DREAM.3D as a 3D matrix where each voxel belonging to a given grain was assigned a unique identifier. This designation enabled direct application of Eq. (3) where pairs of points were randomly placed at increasing separation distances. The resulting empirical SCFs are given in Fig. 2.

B. Spatial Correlation Function

Fitting parameters for each SCF in Sec. II A were found using an unconstrained nonlinear optimization in MATLAB (R2021b) set to a maximum of 10^9 iterations and function evaluations. For the exponential and von Kármán SCFs, the initial guess for the correlation length was a random integer between 0 and 30 μm, noting that the mean grain diameter for all tested microstructures was below 32 μm and the correlation length for the exponential fit was expected to be near the mean grain radius[33]. The initial guess for the Hurst number, κ, was selected as a random number between 0 and 1, per the constraints of the SCF. Given the limited number of fitting parameters for these two functions, the minimization solution was unique, confirmed through 100 iterations of initial conditions. The resulting fits are graphically depicted in Fig. 2. The minimization routine for the summed exponentials SCF required additional constraints to obtain optimal fits. The initial guesses for the pseudo correlation length arguments in the exponents were still constrained to be between 0 and 30 μm. The initial guess for the weighting factors were constrained between -1000 to 1000. Given there are a total of 16 fitting parameters for an eight-term summed exponentials fit, the minimization problem is ill posed. Therefore, through 100 iterations with arbitrary initial guesses, 100 distinct fits were obtained. The correlation lengths were then calculated as the weighted sums of the exponents per Ref.[34].

ACCEPTED MANUSCRIPT

PLEASE CITE THIS ARTICLE AS DOI: 10.1063/5.0091521

Journal of Applied Physics

AIP Publishing

As expected, the summed exponentials SCF provides the lowest fitting error of the empirical data given the large number of fitting parameters, as shown in Figs. 2 and 3. However, this function is highly dependent on the initial conditions used in the optimization routine, particularly for the larger correlation distances, r. The error when using the von Kármán correlation function is improved over the exponential case by nearly an order of magnitude on average. This result is significant given that only one additional fitting parameter is necessary and the fitting solution is unique. Overall, the error is practically independent of distribution width with a slight minimum for a standard deviation $\sim$13 μm.

FIG. 2. Empirical spatial correlation functions (SCFs) for synthetic polycrystalline microstructures with standard deviations of (a) 6.87, (b) 12.72, (c) 16.74, and (d) 20.59 μm with corresponding function fits for exponential, von Kármán, and summed exponential analytical SCFs.

FIG. 3. Sum of squares error for analytical function fits of spatial statistics for various synthetic polycrystalline media as a function of standard deviation. The errorbars for the summed exponential fit corresponds to the minimum and maximum error for 100 iterations of initial guesses for the function fits.

As discussed in Sec. I, correlation length and parameters describing the two point statistics of the microstructure are critical in predicting various material properties[35]. We compare the fitting parameters for the various functions and analyze them relative to the grain size statistics for each microstructure. The correlation length for the summed exponential fits is calculated as the weighted sum of the exponents, as described by Huang et al[34]. First, note

ACCEPTED MANUSCRIPT

PLEASE CITE THIS ARTICLE AS DOI: 10.1063/5.0091521

Journal of Applied Physics

AIP Publishing

that as the distribution width increases, the correlation length proportionally increases for all fitting functions, as shown in Fig. 4. Interestingly, the summed exponentials fits result in correlation lengths practically identical to the single exponential case. Such finding is relevant given the representation for the correlation length in this case has no physical basis. In other words, although the fitting error is minimum for this function, the resulting correlation length does not provide unique information about the microstructure morphology relative to the single exponential function. The von Kármán correlation length was ∼5 μm lower on average independent of distribution width. The second fitting parameter, κ, decreased sharply as the standard deviation increased from 5 to 13 μm but remained relatively constant thenceforth. Recall that the Hurst number represents the roughness of the medium, with a $\kappa = 1$ corresponding to a smooth medium. Despite the microstructure with the lowest standard deviation resulting in a larger total number of sharp grain boundaries, the magnitude of the exponent suggests that the uniformity in the grain size can be treated as smoother perturbations. As the standard deviation increases and the number of small grains rises to ensure volume filling, the Hurst number sharply decreases. Although the number of small grains continues to increase for the larger standard deviations, we hypothesize the presence of the sharper perturbations is accounted for as soon as the grain size distribution deviates from uniformity.

Next we consider the correlation lengths relative to the statistical parameters describing the grain morphology. As expected, for the exponential fit, the correlation length is closest to the mean grain radius (∼15 μm) for the smallest grain size distribution width (i.e., for the microstructure with the most uniform grain size)[12,33]. It is important to note, however, that this is also the distribution width with the greatest fitting error. The correlation lengths quickly deviate from the mean grain radius as the distribution width increases. Therefore, modeling of material response will be significantly impacted if the mean grain radius is used as the correlation length for nonuniform distributions of sizes, as reported elsewhere[1,2]. Other distribution parameters such as the median, mode, and volumetric mean as defined by Arguelles and Turner[1], were also evaluated to determine associations with the correlation length, but none of them were predictive or strongly correlated. Coincidentally, the von Kármán correlation length closely follows the standard deviation for each distribution width. However, this finding is not expected to hold for other mean grain sizes or distribution widths.

ACCEPTED MANUSCRIPT

PLEASE CITE THIS ARTICLE AS DOI: 10.1063/5.0091521

Journal of Applied Physics

AIP Publishing

FIG. 4. Correlation lengths and von Kármán coefficients for best fit solutions of analytical SCFs to empirical data as a function of standard deviation.

C. Ultrasonic Attenuation

Using the analytical fits of the two point statistics, we calculated the attenuation for statistically homogeneous polycrystals with the spatial characteristics obtained from the synthetic polycrystals. In order to confirm that the results were independent of single crystal anisotropy, the attenuation was calculated for two materials with highly different cubic crystal anisotropy, aluminum and lithium. Because the results were nearly identical, only the aluminum results are presented in this section, which were calculated assuming $c_{11} = 108$, $c_{12} = 62$, $c_{44} = 28.3$ GPa, and $\rho = 2700$ kg/m^3.

Figure 5 depicts the normalized longitudinal attenuation where $\bar{L}$ represents the corresponding correlation length for each fitted SCF. Most notably, for the widest distribution given in Fig. 5(d), a number of the attenuation solutions have sudden drop-offs where the attenuation values go negative. These results stem from the numerical instabilities in the fitting procedure but are not identifiable simply by looking at the correlation function of the resulting sum of squares error. One concern arises that these instabilities are only apparent when a wide enough range of frequencies is considered. In other words, if the correlation fit is not restricted for convergence, severe error in attenuation may result from seemingly appropriate SCF fits.

FIG. 5. Normalized longitudinal attenuation for a statistically homogeneous, macroscopically isotropic aluminum polycrystal with spatial statistics defined through synthetic polycrystalline microstructures with standard deviations of (a) 6.87, (b) 12.72, (c) 16.74, and (d) 20.59 μm.

ACCEPTED MANUSCRIPT

PLEASE CITE THIS ARTICLE AS DOI: 10.1063/5.0091521

Journal of Applied Physics

AIP Publishing

In order to enable more quantitative comparison of attenuation, the ratio of attenuations relative to the exponential case are given in Figs. 6 and 7, for longitudinal and shear attenuation, respectively. First, we note that the deviation in the predicted attenuation from the exponential function varies as a function of distribution width, with the sharpest difference observed as the standard deviation in grain size increases from 6.87 to 12.72 μm. For the longitudinal case in Fig. 6, the minimum difference occurs when $k\bar{L} \sim 2$, independent of distribution width, with two instances denoting coinciding values of attenuation for both the von Kármán and summed exponential fits. As expected from the differences observed in the SCF fits in Fig. 2, the attenuation using the summed exponentials fit shows the greatest variation for the 12.72 μm standard deviation in Fig. 6(b). These differences are most apparent at low $k\bar{L}$ values, showing the impact of differences in the correlation function at large r. The von Kármán and summed exponential functions display inverse behavior in relation to the single exponential function, thus, emphasizing the importance of an accurate representation for the SCF when calculating ultrasonic parameters.

FIG. 6. Longitudinal attenuation ratios when using von Kármán and summed exponential SCFs relative to a single exponential fit for an aluminum polycrystal with grain size standard deviations of (a) 6.87, (b) 12.72, (c) 16.74, and (d) 20.59 μm.

The results for the shear attenuation ratios are given in Fig. 7. Interestingly, there is nearly no difference in the attenuation values in the stochastic regime when employing the summed exponentials function relative to the single exponential. In addition, the von Kármán function never coincides with the single exponential term, though the error is also relatively constant in this frequency region. As with the longitudinal attenuation, the error is greatest for the narrowest distribution, in accordance with the errors reported for the SCF fits. It is important to note that in the Rayleigh regime, which is greatly relevant for ultrasonic applications, the difference between the summed exponentials and von Kármán functions for both longitudinal and shear attenuation can be nearly two-fold. It is imperative that the absolute SCF is calculated in realistic materials to determine whether a two

ACCEPTED MANUSCRIPT

PLEASE CITE THIS ARTICLE AS DOI: 10.1063/5.0091521

Journal of Applied Physics

AIP Publishing

parameter function, such as the von Kármán SCF, is suitable to represent the complexities in the heterogeneity of these materials. This work represents a significant first step in this analysis by considering the impact of SCF using realistic synthetic microstructures.

FIG. 7. Shear attenuation ratios when using von Kármán and summed exponential SCFs relative to a single exponential fit for an aluminum polycrystal with grain size standard deviations of (a) 6.87, (b) 12.72, (c) 16.74, and (d) 20.59 μm.

IV. SUMMARY

Describing the microstructure of polycrystalline media through mathematically tractable statistical models is equally desirable and challenging. By analyzing the accuracy of three analytical spatial correlation functions, a critical evaluation of the suitability of these functions to describe polycrystalline media was provided. In this article, synthetic microstructures representative of real metallic polycrystals were generated using open source software. The exact spatial statistics were calculated empirically for four volumes with increasingly wide grain size distributions. Although the summed exponentials approach resulted in minimum fitting error, the numerical instabilities associated with the ill-posed minimization problem suggest more tractable approaches should be explored. To this end, the von Kármán function improved the fit of the two point statistics by nearly an order of magnitude. Furthermore, using different analytical functions to represent the two point statistics resulted in measurable discrepancies in the calculated attenuation exceeding a factor of two. The impact of the SCF on measurable ultrasonic parameters underscores the importance of accurately characterizing polycrystalline microstructures and the challenges posed when seeking to use said metrics as a nondestructive mean of characterization.

ACCEPTED MANUSCRIPT

PLEASE CITE THIS ARTICLE AS DOI: 10.1063/5.0091521

Journal of Applied Physics

AIP Publishing

ACKNOWLEDGMENTS

This material is based upon work supported by the National Science Foundation under Grant No. 2029142. Any opinions, findings, and conclusions or recommendations expressed in this material are those of the authors and do not necessarily reflect the views of the National Science Foundation. Computations for this research were performed on the Pennsylvania State University's Institute for Computational and Data Sciences' Roar supercomputer. The author gratefully acknowledges the assistance of student Tanni Alam Dola in creating the synthetic polycrystals in DREAM.3D.

CONFLICT OF INTEREST

The author has no conflicts to disclose.

AIP PUBLISHING DATA SHARING POLICY

The data that support the findings of this study are available from the corresponding author upon reasonable request.

REFERENCES

[1]A. P. Arguelles and J. A. Turner, "Ultrasonic attenuation of polycrystalline materials with a distribution of grain sizes," The Journal of the Acoustical Society of America **141**, 4347–4353 (2017).

[2]S. T. Abraham, S. Shivaprasad, C. Das, S. Albert, B. Venkatraman, and K. Balasubramaniam, "Effect of grain size distribution on the acoustic nonlinearity parameter," Journal of Applied Physics **127**, 185102 (2020).

[3]D. T. Fullwood, S. R. Niezgoda, and S. R. Kalidindi, "Microstructure reconstructions from 2-point statistics using phase-recovery algorithms," Acta Materialia **56**, 942–948 (2008).

[4]D. T. Fullwood, S. R. Niezgoda, B. L. Adams, and S. R. Kalidindi, "Microstructure sensitive design for performance optimization," Progress in Materials Science **55**, 477–562 (2010).

ACCEPTED MANUSCRIPT

PLEASE CITE THIS ARTICLE AS DOI: 10.1063/5.0091521

Journal of Applied Physics

AIP Publishing

[5]J. G. Berryman, "Measurement of spatial correlation functions using image processing techniques," Journal of Applied Physics **57**, 2374–2384 (1985).

[6]S. R. Kalidindi, S. R. Niezgoda, and A. A. Salem, "Microstructure informatics using higher-order statistics and efficient data-mining protocols," Jom **63**, 34–41 (2011).

[7]P. Altschuh, Y. C. Yabansu, J. Hötzer, M. Selzer, B. Nestler, and S. R. Kalidindi, "Data science approaches for microstructure quantification and feature identification in porous membranes," Journal of Membrane Science **540**, 88–97 (2017).

[8]N. H. Paulson, M. W. Priddy, D. L. McDowell, and S. R. Kalidindi, "Reduced-order structure-property linkages for polycrystalline microstructures based on 2-point statistics," Acta Materialia **129**, 428–438 (2017).

[9]C. M. Kube and A. P. Arguelles, "Pressure influence on elastic wave attenuation in polycrystalline materials," The Journal of the Acoustical Society of America **146**, 4183–4189 (2019).

[10]S. Hirsekorn, "The scattering of ultrasonic waves by multiphase polycrystals," The Journal of the Acoustical Society of America **83**, 1231–1242 (1988).

[11]R. L. Weaver, "Diffusivity of ultrasound in polycrystals," Journal of the Mechanics and Physics of Solids **38**, 55–86 (1990).

[12]F. E. Stanke and G. S. Kino, "A unified theory for elastic wave propagation in polycrystalline materials," The Journal of the Acoustical Society of America **75**, 665–681 (1984).

[13]G. Sha, M. Huang, M. Lowe, and S. Rokhlin, "Attenuation and velocity of elastic waves in polycrystals with generally anisotropic grains: Analytic and numerical modeling," The Journal of the Acoustical Society of America **147**, 2442–2465 (2020).

[14]M. Norouzian and J. A. Turner, "Ultrasonic wave propagation predictions for polycrystalline materials using three-dimensional synthetic microstructures: Attenuation," The Journal of the Acoustical Society of America **145**, 2181–2191 (2019).

[15]M. Norouzian, S. Islam, and J. A. Turner, "Influence of microstructural grain-size distribution on ultrasonic scattering," Ultrasonics **102**, 106032 (2020).

[16]T. Grabec, I. A. Veres, and M. Ryzy, "Surface acoustic wave attenuation in polycrystals: Numerical modeling using a statistical digital twin of an actual sample," Ultrasonics **119**, 106585 (2022).

[17]M. Ryzy, T. Grabec, P. Sedlák, and I. A. Veres, "Influence of grain morphology on ultrasonic wave attenuation in polycrystalline media with statistically equiaxed grains,"

ACCEPTED MANUSCRIPT

PLEASE CITE THIS ARTICLE AS DOI: 10.1063/5.0091521

Journal of Applied Physics

AIP Publishing

The Journal of the Acoustical Society of America **143**, 219–229 (2018).

[18]M. Huang, S. Rokhlin, and M. Lowe, "Finite element evaluation of a simple model for elastic waves in strongly scattering elongated polycrystals," JASA Express Letters **1**, 064002 (2021).

[19]A. Renaud, B. Tie, A.-S. Mouronval, and J.-H. Schmitt, "Multi-parameter optimization of attenuation data for characterizing grain size distributions and application to bimodal microstructures," Ultrasonics **115**, 106425 (2021).

[20]Y. Liu, M. K. Kalkowski, M. Huang, M. J. Lowe, V. Samaitis, V. Cicėnas, and A. Schumm, "Can ultrasound attenuation measurement be used to characterise grain statistics in castings?" Ultrasonics **115**, 106441 (2021).

[21]H. B. Helle, N. H. Pham, and J. M. Carcione, "Velocity and attenuation in partially saturated rocks: poroelastic numerical experiments," Geophysical Prospecting **51**, 551–566 (2003).

[22]H. Sato, M. C. Fehler, and T. Maeda, *Seismic wave propagation and scattering in the heterogeneous earth* (Springer Science & Business Media, 2012).

[23]M. A. Groeber and M. A. Jackson, "Dream. 3d: a digital representation environment for the analysis of microstructure in 3d," Integrating materials and manufacturing innovation **3**, 56–72 (2014).

[24]J. A. Turner, "Elastic wave propagation and scattering in heterogeneous, anisotropic media: Textured polycrystalline materials," The Journal of the Acoustical Society of America **106**, 541–552 (1999).

[25]J. Przybilla, U. Wegler, and M. Korn, "Estimation of crustal scattering parameters with elastic radiative transfer theory," Geophysical Journal International **178**, 1105–1111 (2009).

[26]T.-K. Hong, "Scattering attenuation ratios of p and s waves in elastic media," Geophysical Journal International **158**, 211–224 (2004).

[27]M. Calvet and L. Margerin, "Velocity and attenuation of scalar and elastic waves in random media: A spectral function approach," The Journal of the Acoustical Society of America **131**, 1843–1862 (2012).

[28]S. Torquato, "Exact conditions on physically realizable correlation functions of random media," The Journal of chemical physics **111**, 8832–8837 (1999).

ACCEPTED MANUSCRIPT

PLEASE CITE THIS ARTICLE AS DOI: 10.1063/5.0091521

Journal of Applied Physics

AIP Publishing

[29]S. Torquato, "Necessary conditions on realizable two-point correlation functions of random media," Industrial & engineering chemistry research **45**, 6923–6928 (2006).

[30]A. Van Pamel, G. Sha, M. J. Lowe, and S. I. Rokhlin, "Numerical and analytic modelling of elastodynamic scattering within polycrystalline materials," The Journal of the Acoustical Society of America **143**, 2394–2408 (2018).

[31]C. M. Kube and J. A. Turner, "Acoustic attenuation coefficients for polycrystalline materials containing crystallites of any symmetry class," The Journal of the Acoustical Society of America **137**, EL476–EL482 (2015).

[32]C. M. Kube, "Iterative solution to bulk wave propagation in polycrystalline materials," The Journal of the Acoustical Society of America **141**, 1804–1811 (2017).

[33]F. E. Stanke, "Spatial autocorrelation functions for calculations of effective propagation constants in polycrystalline materials," The Journal of the Acoustical Society of America **80**, 1479–1485 (1986).

[34]M. Huang, G. Sha, P. Huthwaite, S. Rokhlin, and M. Lowe, "Longitudinal wave attenuation in polycrystals with elongated grains: 3d numerical and analytical modeling," The Journal of the Acoustical Society of America **149**, 2377–2394 (2021).

[35]P. B. Corson, "Correlation functions for predicting properties of heterogeneous materials. i. experimental measurement of spatial correlation functions in multiphase solids," Journal of applied Physics **45**, 3159–3164 (1974).

AIP Publishing

Journal of Applied Physics

ACCEPTED MANUSCRIPT

PLEASE CITE THIS ARTICLE AS DOI: 10.1063/5.0091521

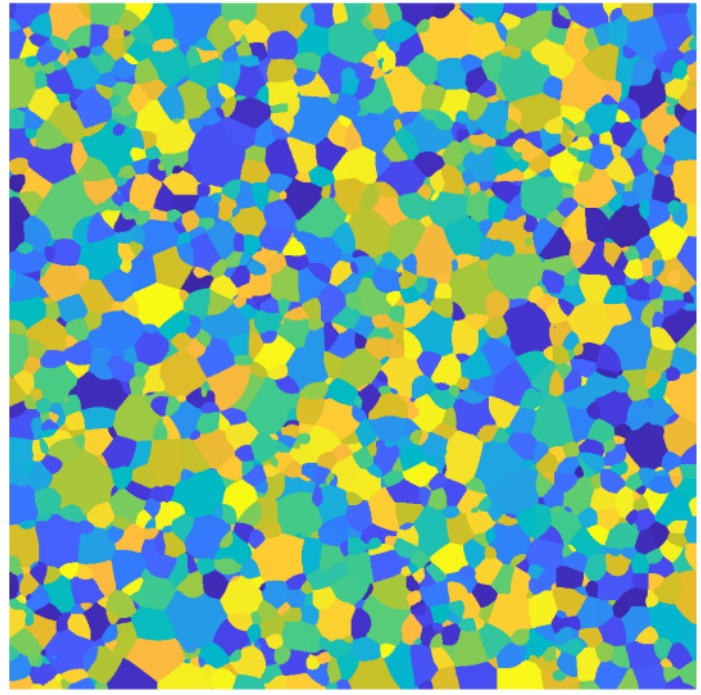

AIP Publishing

Journal of Applied Physics

ACCEPTED MANUSCRIPT

PLEASE CITE THIS ARTICLE AS DOI: 10.1063/5.0091521

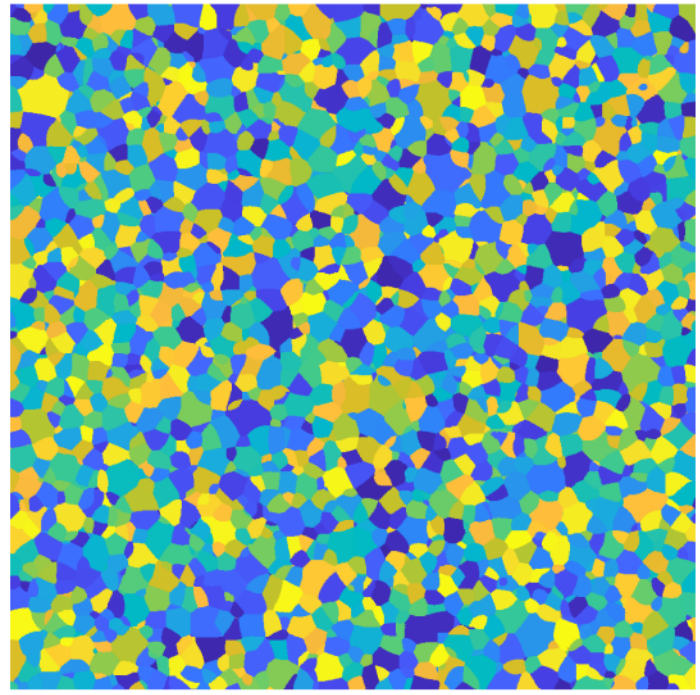

AIP Publishing

Journal of Applied Physics

ACCEPTED MANUSCRIPT

PLEASE CITE THIS ARTICLE AS DOI: 10.1063/5.0091521

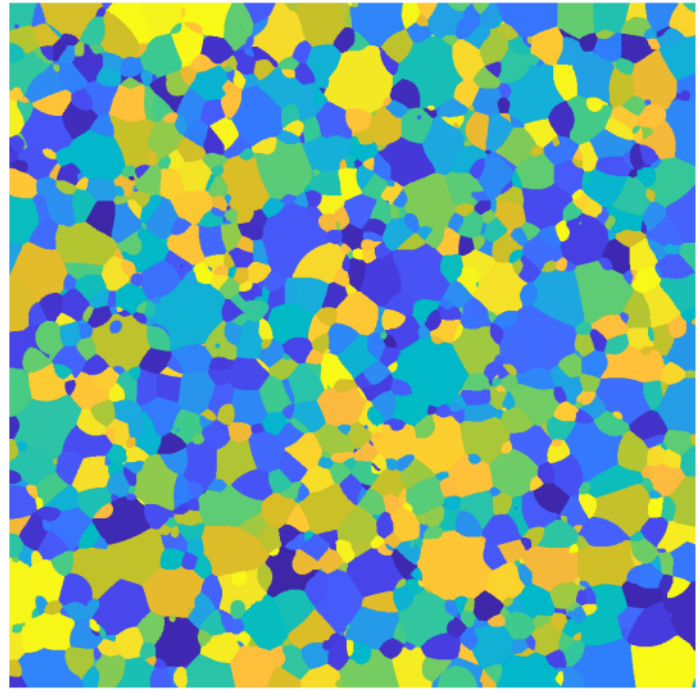

AIP Publishing

Journal of Applied Physics

ACCEPTED MANUSCRIPT

PLEASE CITE THIS ARTICLE AS DOI: 10.1063/5.0091521

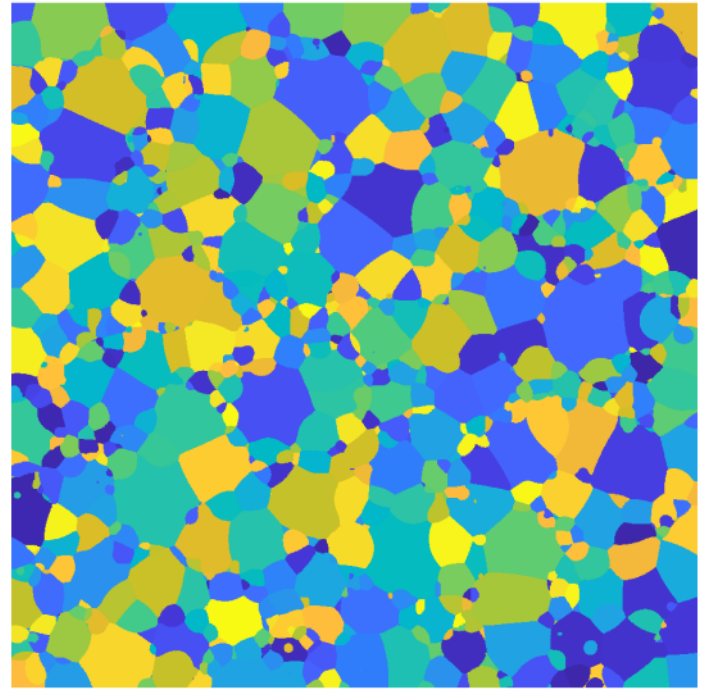

AIP Publishing
Journal of Applied Physics
ACCEPTED MANUSCRIPT
PLEASE CITE THIS ARTICLE AS DOI: 10.1063/5.0091521

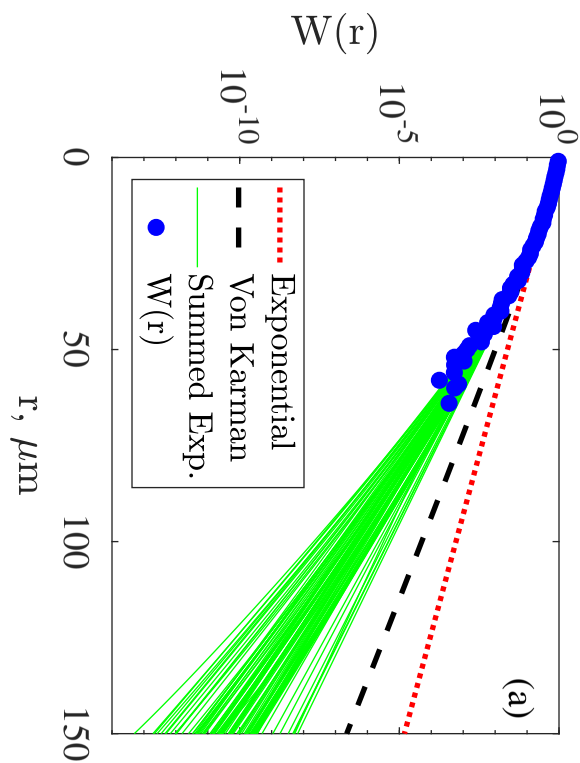

Journal of Applied Physics

ACCEPTED MANUSCRIPT

PLEASE CITE THIS ARTICLE AS DOI: 10.1063/5.0091521

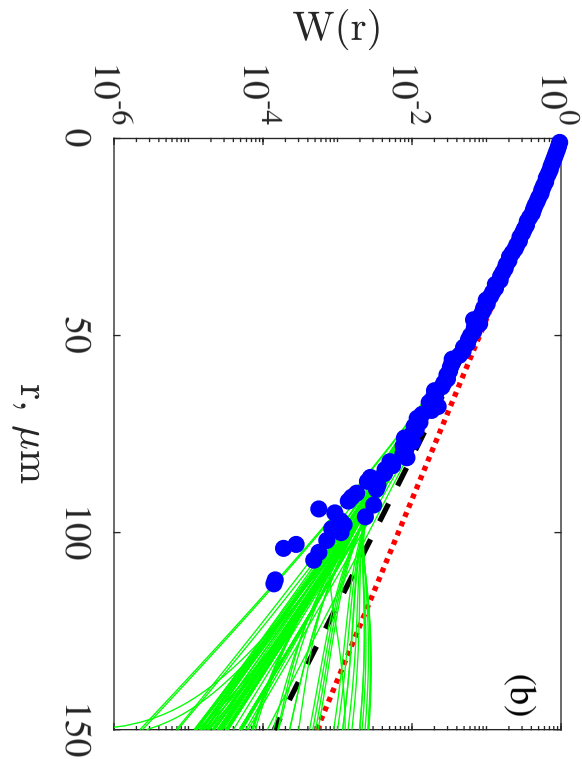

Journal of Applied Physics

ACCEPTED MANUSCRIPT

PLEASE CITE THIS ARTICLE AS DOI: 10.1063/5.0091521

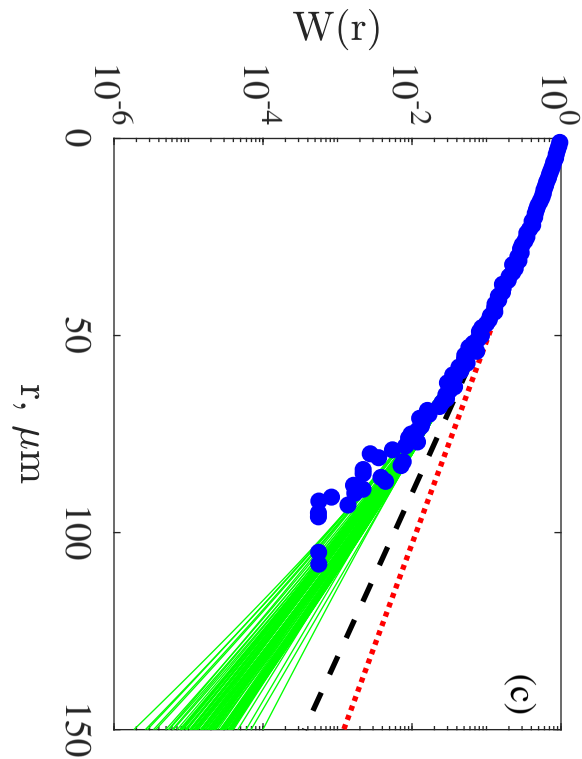

Journal of Applied Physics

ACCEPTED MANUSCRIPT

PLEASE CITE THIS ARTICLE AS DOI: 10.1063/5.0091521

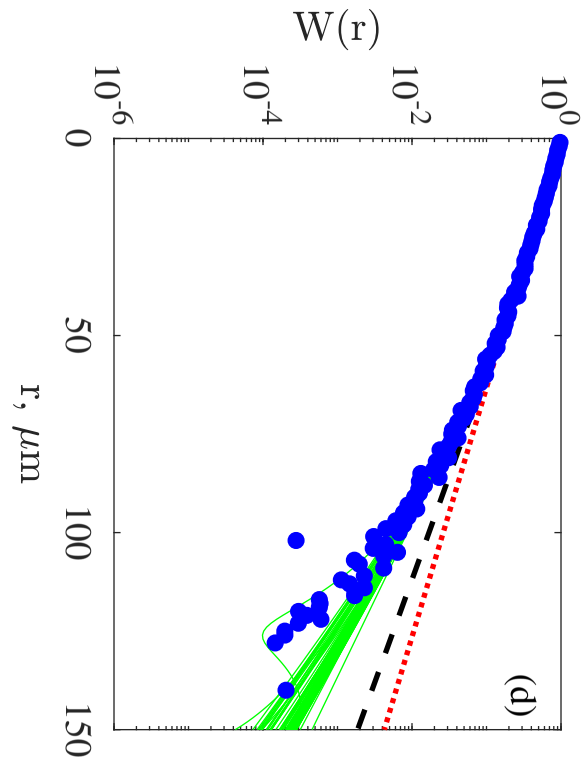

ACCEPTED MANUSCRIPT

Journal of Applied Physics

PLEASE CITE THIS ARTICLE AS DOI: 10.1063/5.0091521

AIP Publishing

Journal of Applied Physics

ACCEPTED MANUSCRIPT

PLEASE CITE THIS ARTICLE AS DOI: 10.1063/5.0091521

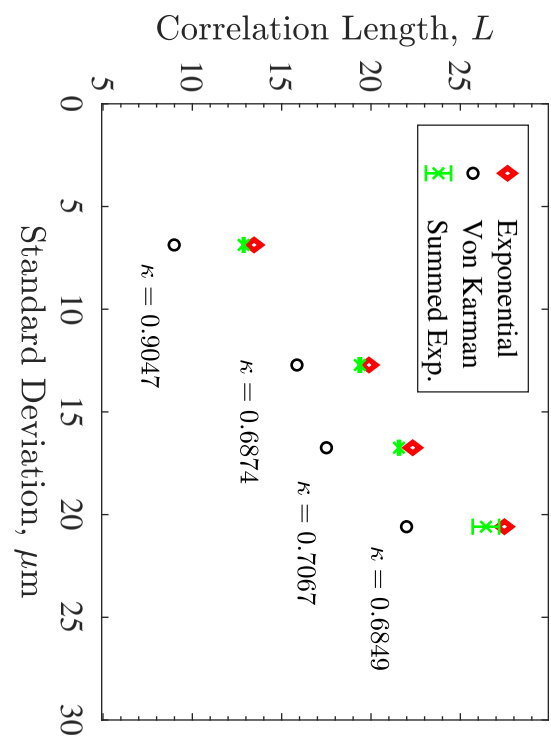

AIP Publishing
Journal of Applied Physics

ACCEPTED MANUSCRIPT

PLEASE CITE THIS ARTICLE AS DOI: 10.1063/5.0091521

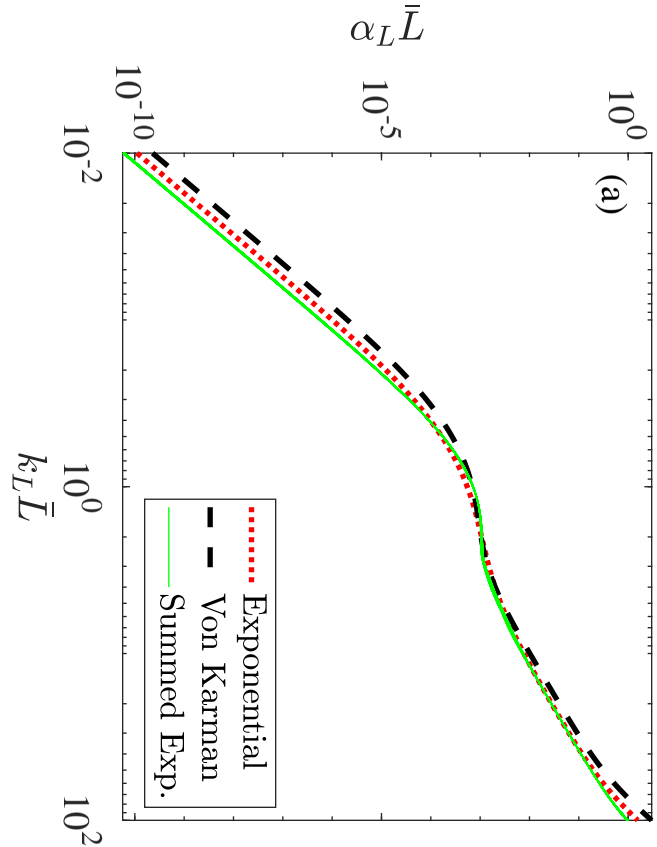

AIP Publishing
Journal of Applied Physics

ACCEPTED MANUSCRIPT

PLEASE CITE THIS ARTICLE AS DOI: 10.1063/5.0091521

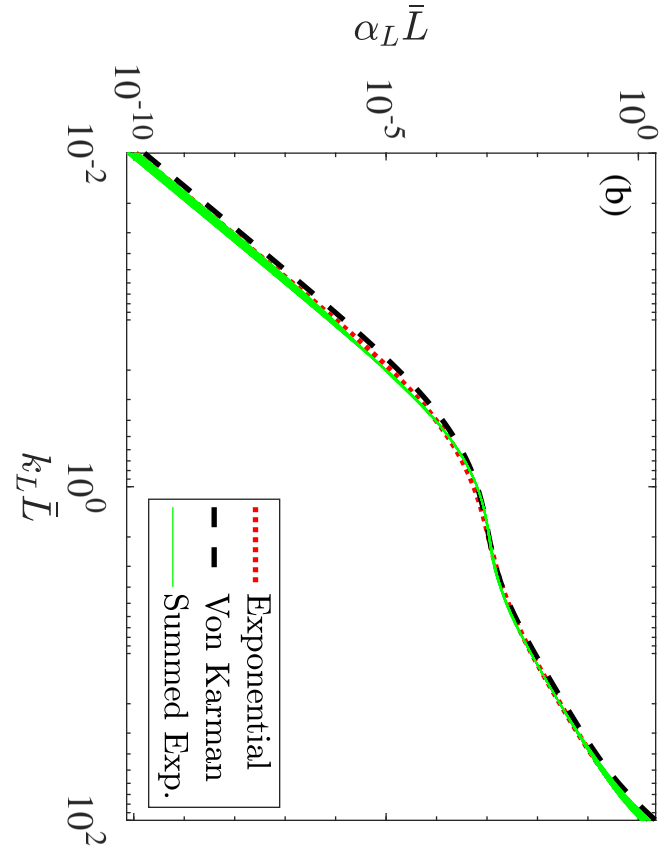

AIP Publishing
Journal of Applied Physics

ACCEPTED MANUSCRIPT

PLEASE CITE THIS ARTICLE AS DOI: 10.1063/5.0091521

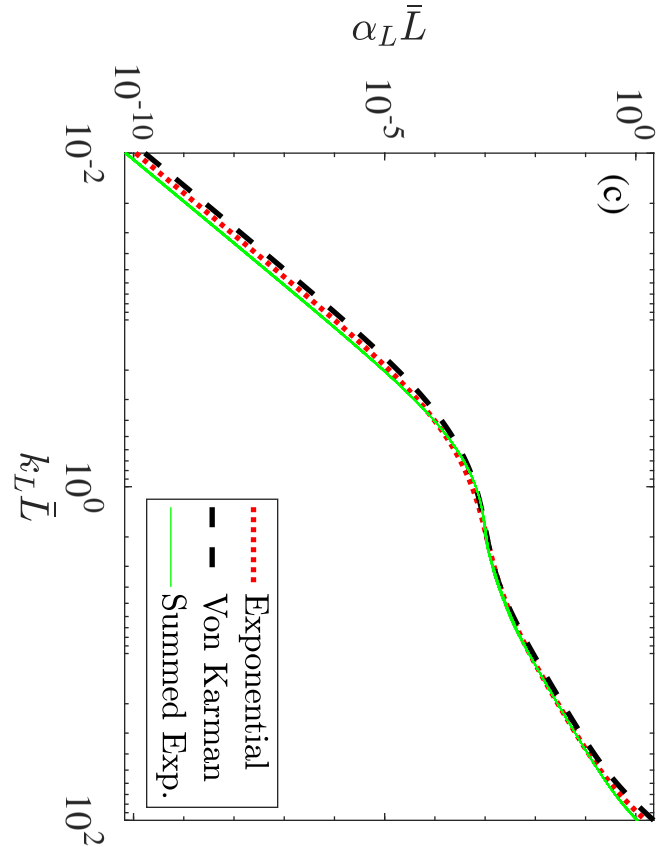

AIP Publishing

Journal of Applied Physics

ACCEPTED MANUSCRIPT

PLEASE CITE THIS ARTICLE AS DOI: 10.1063/5.0091521

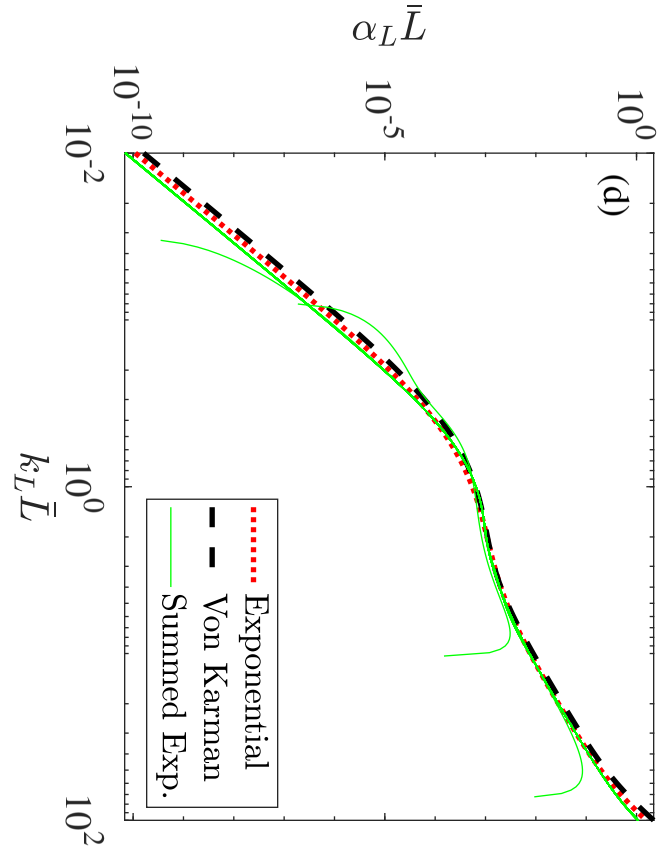

AIP Publishing
Journal of Applied Physics

ACCEPTED MANUSCRIPT

PLEASE CITE THIS ARTICLE AS DOI: 10.1063/5.0091521

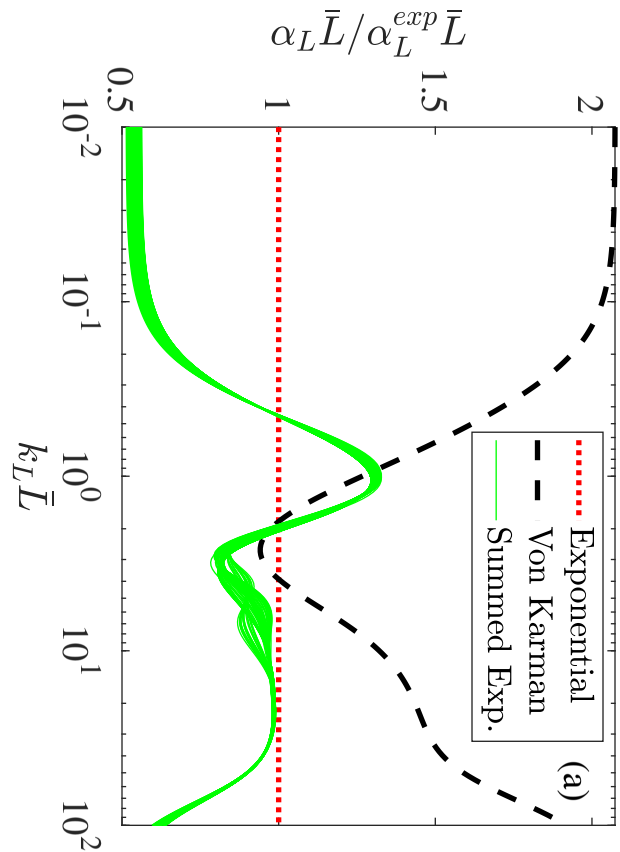

AIP Publishing
Journal of Applied Physics
ACCEPTED MANUSCRIPT
PLEASE CITE THIS ARTICLE AS DOI: 10.1063/5.0091521

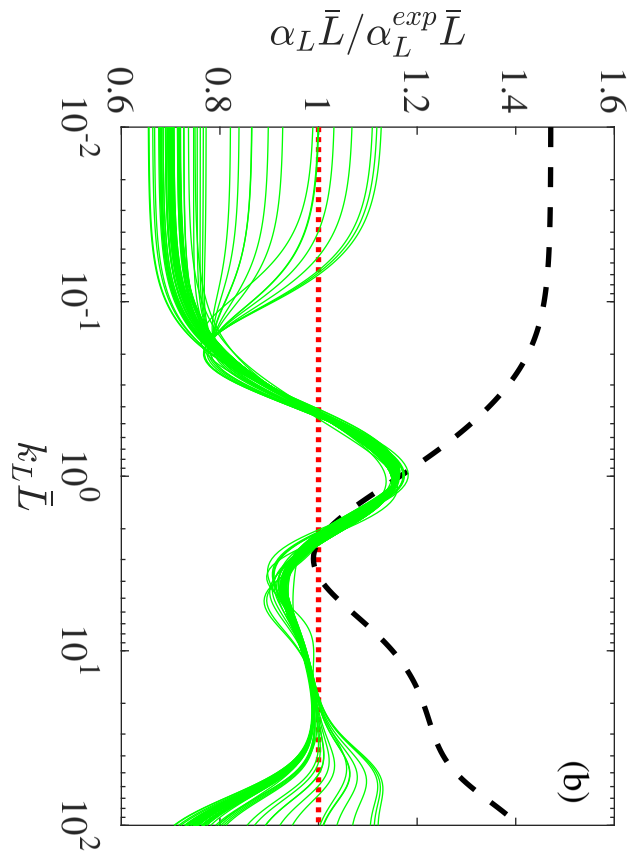

AIP Publishing
Journal of Applied Physics
ACCEPTED MANUSCRIPT
PLEASE CITE THIS ARTICLE AS DOI: 10.1063/5.0091521

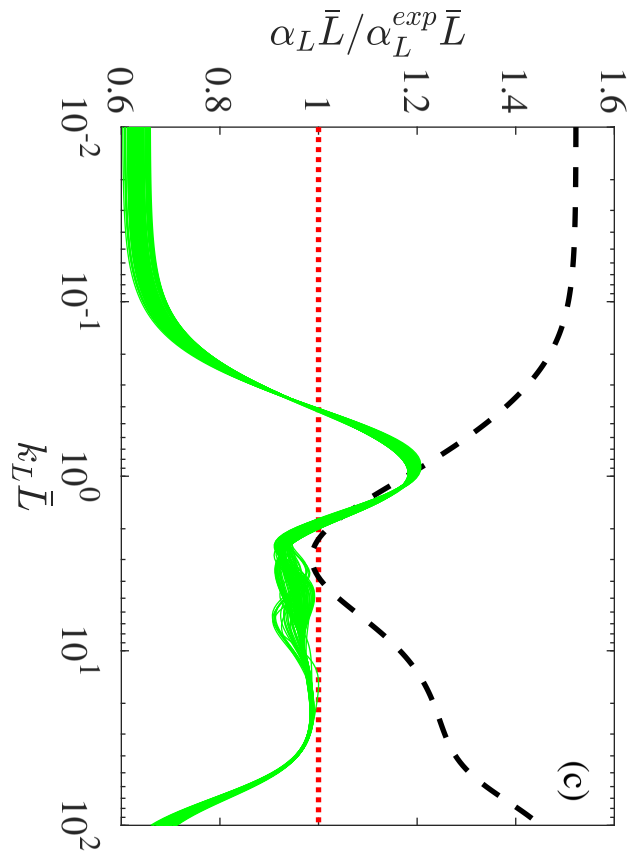

AIP Publishing
Journal of Applied Physics
ACCEPTED MANUSCRIPT
PLEASE CITE THIS ARTICLE AS DOI: 10.1063/5.0091521

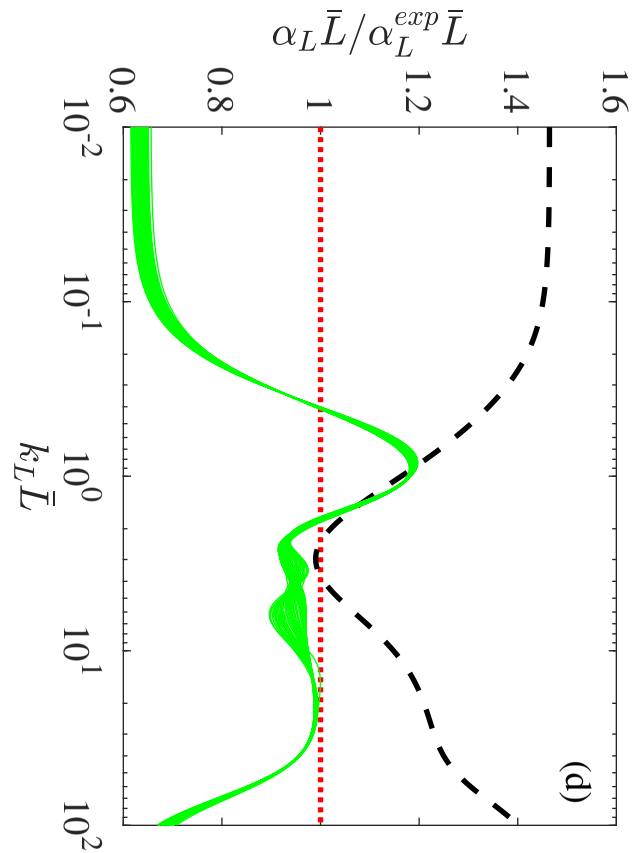

AIP Publishing

Journal of Applied Physics

ACCEPTED MANUSCRIPT

PLEASE CITE THIS ARTICLE AS DOI: 10.1063/5.0091521

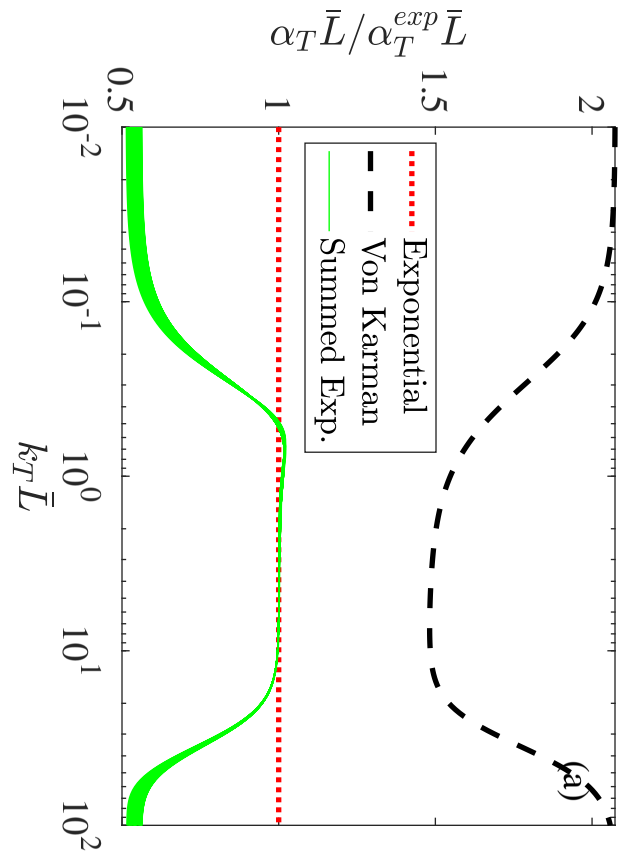

AIP Publishing

Journal of Applied Physics

ACCEPTED MANUSCRIPT

PLEASE CITE THIS ARTICLE AS DOI: 10.1063/5.0091521

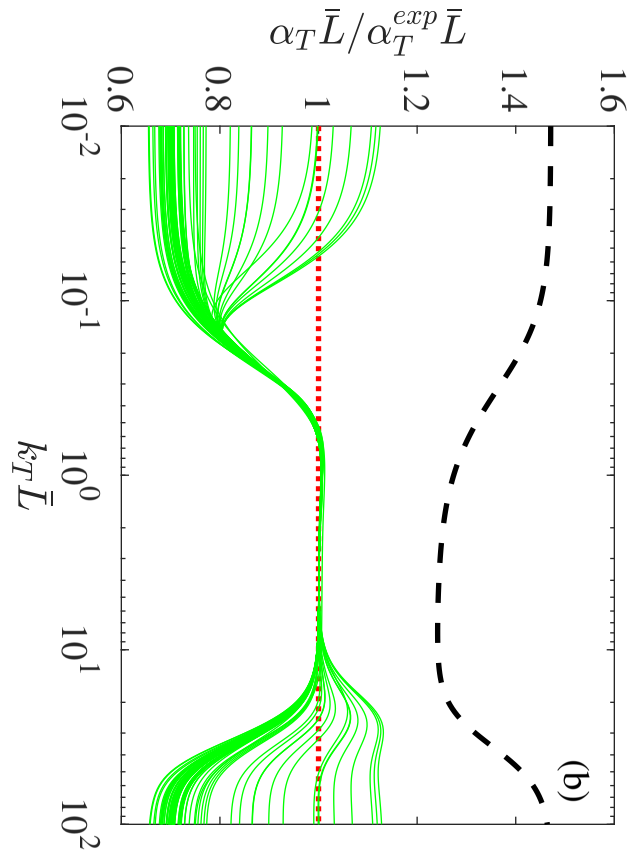

AIP Publishing
Journal of Applied Physics

ACCEPTED MANUSCRIPT

PLEASE CITE THIS ARTICLE AS DOI: 10.1063/5.0091521

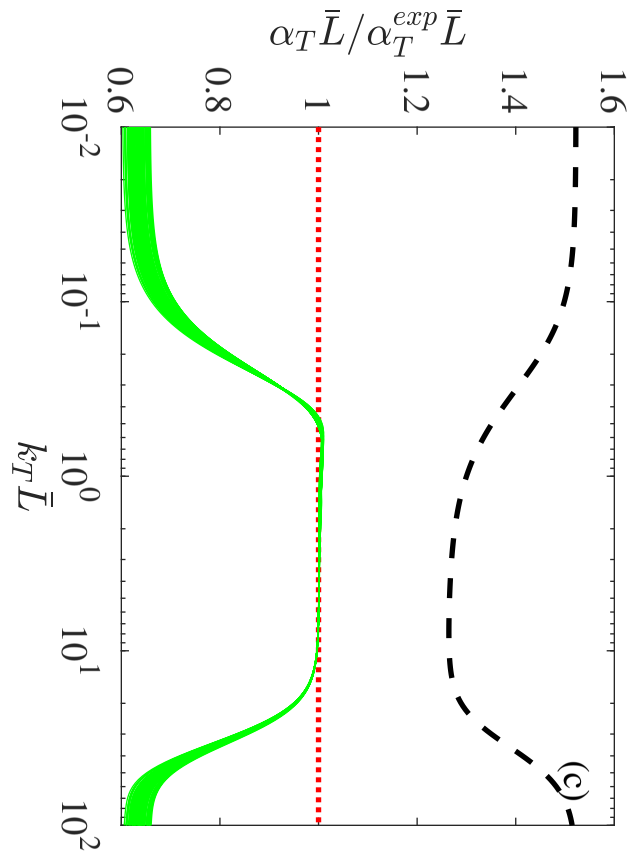

AIP Publishing
Journal of Applied Physics
ACCEPTED MANUSCRIPT
PLEASE CITE THIS ARTICLE AS DOI: 10.1063/5.0091521